Available at https://www.iasj.net/iasj

Iraqi Academic Scientific Journals

Journal homepage:
https://journals.uokerbala.edu.iq/index.php/UOKJ

Research Article

A study of Thermal Imaging technique for system operates with different apertures

Fatima Raheem Kalaf * Azhr Abdulzahraa Raheem*

* Physics of Department, College of Science, Kerbala University, Karbala, Iraq

Article Info

Article history:

Received 8-6-2023

Received in revised form 20-6-2023

Accepted 20-6-2023

Available online13-12 -2023

Keywords: Thermal imaging, intensity distribution, Atmospheric transmission of IR,detection and recognition object.

Abstract:

Thermal imaging is very important because it has many significant and useful applications. The principle of its work is based on capturing infrared rays from objects, leading to detect all objects that emit infrared rays when their temperature is higher than absolute zero degrees. This paper aims to study the intensity distribution of the thermal image by using an optical system that operates with different shapes of the enter apertures and investigate the efficiency of detected thermal image to obtain a better possible detected thermal image for moving targets. The effect of the circular, square, and triangular apertures on the intensity distribution of detected thermal images of moving targets at different speeds was studied. An ideal optical system (free aberration) is considered in this research. Comparison between each aperture is performed to find out which of these apertures (circular, square, triangular) gives a better thermal image quality. This is evidence of the effectiveness of using the triangular aperture to detect moving objects by thermal optical systems.

Corresponding Author E-mail: azhr.a@uokerbala.edu.iq

Peer review under responsibility of Iraqi Academic Scientific Journal and University of Kerbala.

INTRODUCTION

The photography technique is one of the best inventions of science in the documentation process. This technique allowed objective documentation for many conditions. In general, images were used mainly for documentation, clarification, and interpretation of the observed phenomena. Because of the rapid progress in this technology, the concept of the imaging technique has been developed to include more advanced and useful performance. Whereas, personal computers and workstations are helpful and good enough to handle image data processing [1].

The thermal imaging technology was initially used in particular by the military as a detection method and surveillance for military purposes. Nowadays, it has become more spread in many fields and thus has a wider range of applications [2,3].

Thermal imaging technology is considered one of the best and very powerful remote sensing techniques, as it collects the required data to produce a thermal image of the target quickly and with high efficiency. So, it also has been used mainly in field studies related to the environment [3,4].

Thermal imaging technology is more advantageous compared to visual imaging technology because thermal radiation can detect through dark, smoke, fog, and dust. This is performed by collecting the IR radiation in completely dark weather compared to visible radiation in normal optical systems. So the targets can be detected in all weather conditions and different environments because it depends on the amount of heat that the target emits [3,5].

In general, formed images are not completely perfect due to the optical system suffers from many defects that distort the captured image such as aberrations and diffractions. The main reason for aberrations in the formed image is the wave nature of light, which is usually affected by many different factors. The shape of the aperture that is used and the shape of the object (a line, a point, or an edge) are factors that may affect the quality of the detected image [6,7].

Calculation of spread functions, which represents the descriptions of the intensity distribution in the image plane for a specific object (edge, line, and point), indicates a way to evaluate the accuracy of the detected image by an optical system. These functions depend on the amount and type of aberrations occurring in the optical system, leading to inferring the quantity of diffractions and aberrations resulting from a used aperture in the optical system. Thus, the calculation of such functions is one of the important techniques in the process of determining the efficiency of the optical system [8–10].

In this paper, the effect of the shape of the used aperture in the optical system is studied by calculating the intensity distribution of the detected thermal image (image clarity). Where the shape of the used aperture in the optical system represents an important aspect that affects the intensity distribution in the image plane of detected images [6].

THEORY CONSIDERATION

In this work, a new spread function was considered for rectangular objects which is similar to the shape of different vehicles, known as the rectangular spread function (RSF).

Rectangular objects were selected because such objects (vehicles) are common in military applications for the purpose of surveillance and border security. This function is used to model the intensity distribution in the image plane of an optical system that operates with different shapes of enter aperture.

Rectangular objects are two-dimensional objects consisting of two dimensions of length and width represented by the dimensions (A, B) that contain infinite point sources of non-homogeneous illumination.

Thus, by making a double integral of the point spread function and multiplying with the intensity function of the rectangular object, the intensity distribution for the rectangular image (rectangular spread function) is produced as follows [11]:

$$R(z\backslash, m\backslash) = \int_{-\infty}^{\infty}\int_{-\infty}^{\infty} R(z,m).G(z\backslash - z, m\backslash - m)dzdm \quad 1$$

Where (z,m) and (z\,m\) are the dimensionless coordinates in the object and image plane, respectively. R(z,m) is the distribution spectrum of the rectangular object, and G(z\-z,m\-m) represents the point spread function resulting from a single source at the rectangular object.

From the equation of the point spread function [12]:

$$G(z\backslash, m\backslash) = \int_y \int_{y_1} \int_x \int_{x_1} f(x,y)\cdot e^{i(z\backslash x + m\backslash y)} f^*(x_1,y_1)\cdot e^{i(z\backslash x_1 + m\backslash y_1)} dx_1 dx dy_1 dy \quad 2$$

we can write [13]:

$$G(z\backslash - z, m\backslash - m) = \int_y \int_{y_1} \int_x \int_{x_1} f(x,y).f^*(x_1,y_1)\cdot e^{i(z\backslash + z)(x-x_1)} .$$
$$e^{i(m\backslash + m)(y-y_1)} dx_1 dx dy_1 dy \quad 3$$

By substituting eq. 3 in eq. 1 we get:

$$R(z\backslash, m\backslash) = \int_{-\infty}^{\infty}\int_{-\infty}^{\infty}\int_y\int_{y_1}\int_x\int_{x_1} R(z,m).f(x,y).f^*(x_1,y_1)$$
$$\cdot e^{i(z\backslash + z)(x-x_1)}.e^{i(m\backslash + m)(y-y_1)} dx_1 dx dy_1 dy\, dzdm \quad 4$$

The distribution spectrum of the rectangular object is determined by the following conditions [14]:

$$R(z,m) = 1 \quad for \quad \begin{Bmatrix} z\ or\ m & \leq A \\ z\ or\ m & \leq B \end{Bmatrix}$$
$$R(z,m) = 0 \quad for \quad \begin{Bmatrix} z\ or\ m & > A \\ z\ or\ m & > B \end{Bmatrix}$$

Where A and B are the main axes of the rectangular object, so equation (4) becomes:

$$R(z\backslash, m\backslash) = \int_y\int_{y_1}\int_x\int_{x_1} f(x,y).f^*(x_1,y_1).e^{iz\backslash(x-x_1)}.e^{im\backslash(y-y_1)} dx_1 dx dy_1 dy$$
$$\int_{-A}^{+A} e^{iz(x-x_1)} dz \int_{-B}^{+B} e^{im(y-y_1)} dm \quad 5$$

Using Mathematical relation, the last two integrals in equation 5 can be written as [13]:

$$\int_{-A}^{+A} e^{iz(x-x_1)} dz = \frac{\sin[(x-x_1)A]}{(x-x_1)} \quad 6$$

$$\int_{-B}^{+B} e^{im(y-y_1)} dm = \frac{\sin[(y-y_1)B]}{(y-y_1)} \quad 7$$

From equations 5, 6, and 7, the rectangular spread function can be expressed as:

$$R(z\backslash, m\backslash) =$$
$$\int_y\int_{y_1}\int_x\int_{x_1} f(x,y).f^*(x_1,y_1).e^{iz\backslash(x-x_1)}.e^{im\backslash(y-y_1)} \frac{\sin[(x-x_1)A]}{(x-x_1)} . \frac{\sin[(y-y_1)B]}{(y-y_1)} dx_1 dx dy_1 dy \quad 8$$

Since the intensity distribution at the image level is symmetrical, therefore, only one coordinate is taken (z\), so the coordinate (m\) assume to be equal to zero. f(x, y) is the pupil function, which is defined within the used aperture and equal to [15]:

$$f(x,y) = \tau(x,y)e^{ikw(x,y)} \quad for\ inside\ aperture$$
$$f(x,y) = 0 \quad for\ outside\ aperture$$

Where: K is the wave number and equal to $2\pi/\lambda$, and λ is the wavelength of the applied source. W(x,y) is the aberration function .τ represents the transparency of the exit pupil and is equal to one for the uniform aperture. As a result, the integral's limits -∞ to +∞ are limited by the used aperture [15].
After substituting(f, f^*)in equation8,it results:

$$R(z\backslash) = \int_y \int_{y_1} \int_x \int_{x_1} e^{iz\backslash(x-x_1)+ikw(x,y)-ikw(x_1,y_1)} \frac{\sin[(x-x_1)A]}{(x-x_1)} . \frac{\sin[(y-y_1)B]}{(y-y_1)} dx_1 dx dy_1 dy \quad 9$$

But:

$$e^{iz\backslash(x-x_1)+ikw(x,y)-ikw(x_1,y_1)} = \cos\{z\backslash(x-x_1) + kw(x,y) - kw(x_1,y_1)\} + i\sin\{z\backslash(x-x_1) + kw(x,y) - kw(x_1,y_1)\}$$

Since the intensity is real, therefore the imaginary part of the above equation must be equal to zero, thus:

$$R(z\backslash) = N \int_y \int_{y_1} \int_x \int_{x_1} cos\{k[w(x,y) - w(x_1,y_1)] + z'(x-x_1)\} . \frac{\sin[(x-x_1)A]}{(x-x_1)} . \frac{\sin[(y-y_1)B]}{(y-y_1)} dx_1 dx dy_1 dy \quad 10$$

For an ideal system $w(x,y)$=0, thus, the last equation becomes:

$$R(z\backslash) = N \int_y \int_{y_1} \int_x \int_{x_1} cos\{z'(x-x_1)\} . \frac{\sin[(x-x_1)A]}{(x-x_1)} . \frac{\sin[(y-y_1)B]}{(y-y_1)} dx_1 dx dy_1 dy \quad 11$$

The last equation (10) represents the formula of the rectangular spread function (RSF), where A and B: represent the length and width of the rectangle object, N is the normalized factor whose value can calculate when z=0, and R(z\)=1.

By including the effect of the linear motion factor the equation of the rectangular spread function becomes as [13]:

$$R(z\backslash) = N \int_y \int_{y_1} \int_x \int_{x_1} cos\{z'(x-x_1)\} . \frac{\sin[(x-x_1)A]}{(x-x_1)} . \frac{\sin[(y-y_1)B]}{(y-y_1)} \frac{\sin(\pi L(x-y))}{\pi L(x-y)} dx_1 dx dy_1 dy \quad 12$$

Where L: is the linear motion factor, which can be presented as [16]:

$$L = \frac{t_e v_i}{\lambda F^{\neq}} \quad 13$$

t_e : is the snapshot time, and for the used thermal camera equal to $t_e = \frac{1}{25}\ sec.$
λ: The used infrared wavelength, which is for used the thermal camera is $\lambda = 10\mu m$.
$F^{\neq}$: is the optical system focal number, which for used thermal camera is equal to 18.
f: is the lens focal length of the thermal camera and it is equal to 36 mm.

v_i : is the image motion and can be found from the following relationship:

$\frac{v_0}{v_i} = \frac{R}{f}$ or $v_i = \frac{f v_0}{R}$

Where:

v_0: is the speed of the object's motion and was determined for a moving target at different speeds in this research.

Finally, the RSF equation (11) can be written depending on the shape of the used aperture, where the area of each aperture is considered as the same area and equal to π.

1. RSF equation for Circular Aperture:

$$R(z') = N \int_{-1}^{1} \int_{-1}^{1} \int_{-\sqrt{1-y^2}}^{\sqrt{1-y^2}} \int_{-\sqrt{1-y1^2}}^{\sqrt{1-y1^2}} \cos z'(x - x_1) \frac{\sin[(x-x_1)A]}{(x-x_1)} \frac{\sin[(y-y_1)B]}{(y-y_1)} \frac{\sin(\pi L(x-y))}{\pi L(x-y)} dx_1 dx dy_1 dy \quad (14)$$

2. RSF equation for Square Aperture:

$$R(z') = N \int_{-\frac{\sqrt{\pi}}{2}}^{\frac{\sqrt{\pi}}{2}} \int_{-\frac{\sqrt{\pi}}{2}}^{\frac{\sqrt{\pi}}{2}} \int_{-\frac{\sqrt{\pi}}{2}}^{\frac{\sqrt{\pi}}{2}} \int_{-\frac{\sqrt{\pi}}{2}}^{\frac{\sqrt{\pi}}{2}} \cos z'(x - x_1) \frac{\sin[(x-x_1)A]}{(x-x_1)} \frac{\sin[(y-y_1)B]}{(y-y_1)} \frac{\sin(\pi L(x-y))}{\pi L(x-y)} dx_1 dx dy_1 dy \quad (15)$$

3. RSF equation for Triangular Aperture:

$$R(z') = N \int_{-1.16}^{1.16} \int_{-1.16}^{1.16} \int_{-\frac{y-1.66}{\sqrt{3}}}^{\frac{y-1.66}{\sqrt{3}}} \int_{-\frac{y1-1.66}{\sqrt{3}}}^{\frac{y1-1.66}{\sqrt{3}}} \cos z'(x - x_1) \frac{\sin[(x-x_1)A]}{(x-x_1)} \frac{\sin[(y-y_1)B]}{(y-y_1)} \frac{\sin(\pi L(x-y))}{\pi L(x-y)} dx_1 dx dy_1 dy \quad (16)$$

RESULT AND DISCUSSION

In this section, the spread function for a rectangular object is calculated for vehicles moving at different speeds (40,80,120 Km/h) and at different linear distances (250, 500, 750, 1000, 1500, 2000, 3000, 4000 m). The used optical system is a free aberration optical system that works with different apertures. Circular, square, and triangular apertures are considered for the optical system to find out the intensity distribution of the detected thermal image for the optical system operating with the three apertures. Comparing the images that were produced for each of these three apertures to see which one is more appropriate and suitable in the process of producing thermal images for moving vehicles.

In this paper, an investigation of one of the most important factors that affect the intensity of the thermal image of the target is the

velocity and the direction of the moving target is performed.

Figure 1 represents the intensity distribution of the detected thermal image of a vehicle moving at 40 Km/h, for a system operating with a circular aperture. All curves represent the intensity distribution of the rectangular thermal image at the image plane. It is clear that the RSF curves comprise a main peak starting at a higher value and begin to decrease whatever the distances between the camera and target increase. One can observe that a vehicle at a distance of (250 m) has the best quality compared to the other distances. As, in this case, the detected thermal image has a high value of intensity, leading to getting a high-clarity thermal detected image that can be recognized and distinguished evidently. Figures 2 and 3 have also the same behavior as Figure 1 with decreases in the values of RSF peaks. This is due to the effect of the velocity of the observed object for the same optical system and the same distances.

Figures 4, 5, and 6 represent the intensity distribution of the detected thermal image of a vehicle moving at 40, 80, and 120 Km/h, for a system operating with a square aperture, respectively. From the figures, the effect of target velocity is clear as well in this case. Where the intensity value decreases with the increase of the distance at which the vehicle is located. As well as the increase in the speed at which the vehicle moves leads to a decrease in the clarity of the detected image due to decreasing in the intensity value of the RSF peak.

The same optical behavior is found for the case when triangular aperture is used as shown in figures Figure 7, 8, 9. In addition, it is noticeable that the better intensity value is at a distance of 500 m when the speed of the vehicle is high. Thus, one can predict that the appropriate range to produce a good thermal image of a vehicle moving at a high speed is at distances more than 500 m for all apertures (circular, square, and triangular) of the used optical system.

Generally, from all cases of velocity and distances, at the range 250-750m the target can be distinguished and a clear image can be detected. Moreover, at 750-1000m which can distinguish the target, but it is not as accurate as the image that was produced at the range of 250-750 m. For the range of 1000-2000m the target is difficult to distinguish, while in the range of more than 3000 m, the image is almost non-existent.

Fig. 10 shows a comparison between the intensity distribution of the detected thermal image of an object with linear motion of 40 Km/h for systems operating with different apertures (circular, square, triangular). Distance values of objects are considered as (250, 500, 750, 1000, 2000, 3000, and 4000) m for different apertures.

Due to the maximum values of the intensity, it is clear that the best detected thermal image obtained from the system works using the triangular aperture. This could be due to reducing the entry rays to the optical system which helps in decreasing the diffraction effects. As well as the best distance of detection is 250 m for all apertures.

The comaparison of detected thermal image of a vehicle moving at a speed of 80 and 120 Km/h is presented in Fig. 11, and Fig. 12 respectively. It is obvious that the triangular aperture still gives the best intensity values over distances in case of less than 2 Km. This range of detection (less than 2 Km) is the effective distance for the recognition of an image with good quality. Thus, one can say that the triangular aperture is the best aperture for moving objects compared to the other apertures under study. Additionally, the best distance for detecting the thermal image, in the case where the linear motions are 80 and 120 Km/h, is at a distance of 500 m. This indicates that increasing the linear motion leads to a decrease in the effective distance of image detection. This is clear from Fig. 12 where the effective distance of detection is even higher than 500 m, All mentioned valued, which are in the figures 10, 11 12, are listed in tables 1, 2 , 3, respectively.

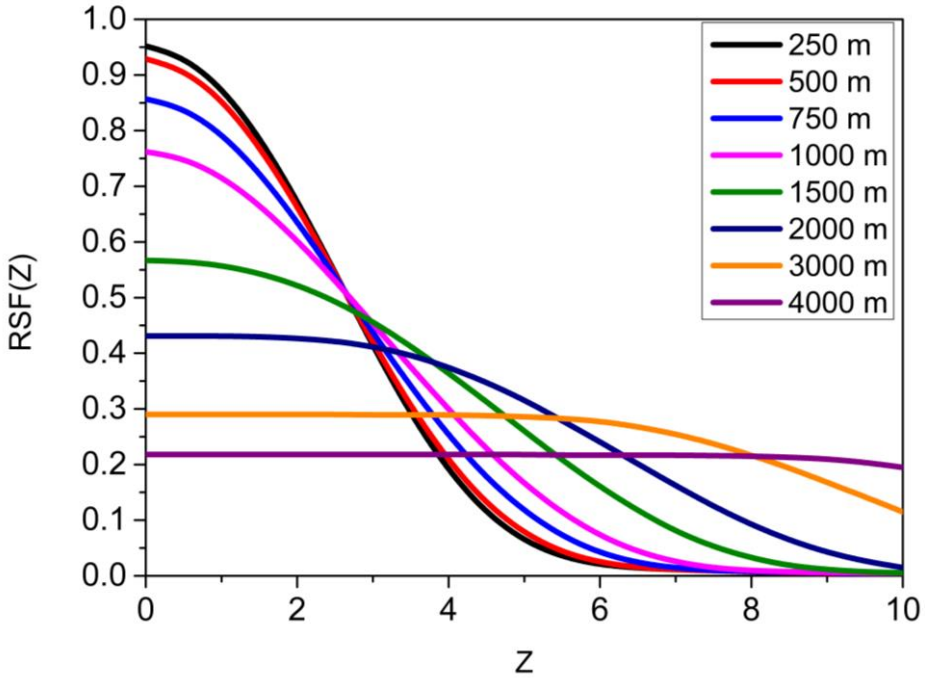

Figure 1. The intensity distribution of the detected thermal image of a vehicle moving at 40 Km/h for a system operating with a circular aperture.

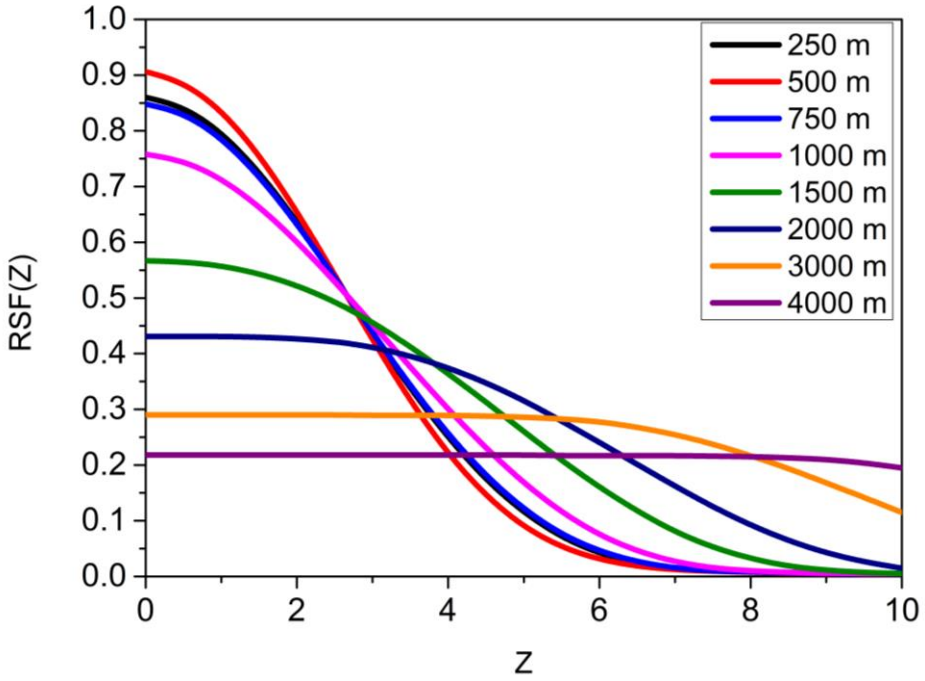

Figure 2. The intensity distribution of the detected thermal image of a vehicle moving at 80 Km/h for a system operating with a circular aperture.

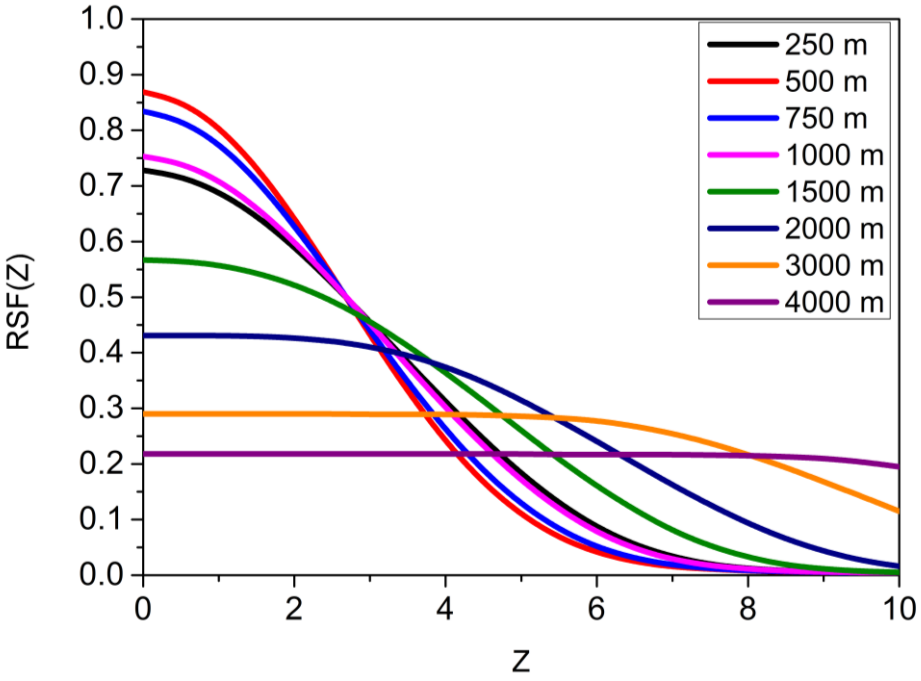

Figure 3. The intensity distribution of the detected thermal image of a vehicle moving at 120 Km/h for a system operating with a circular aperture.

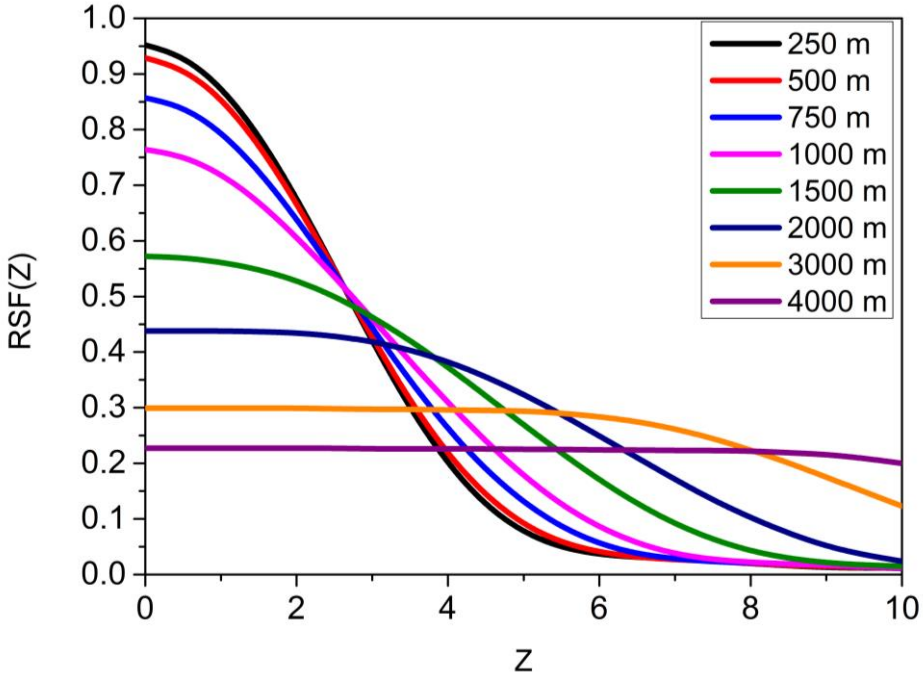

Figure 4. The intensity distribution of the detected thermal image of a vehicle moving at 40 Km/h for a system operating with a square aperture.

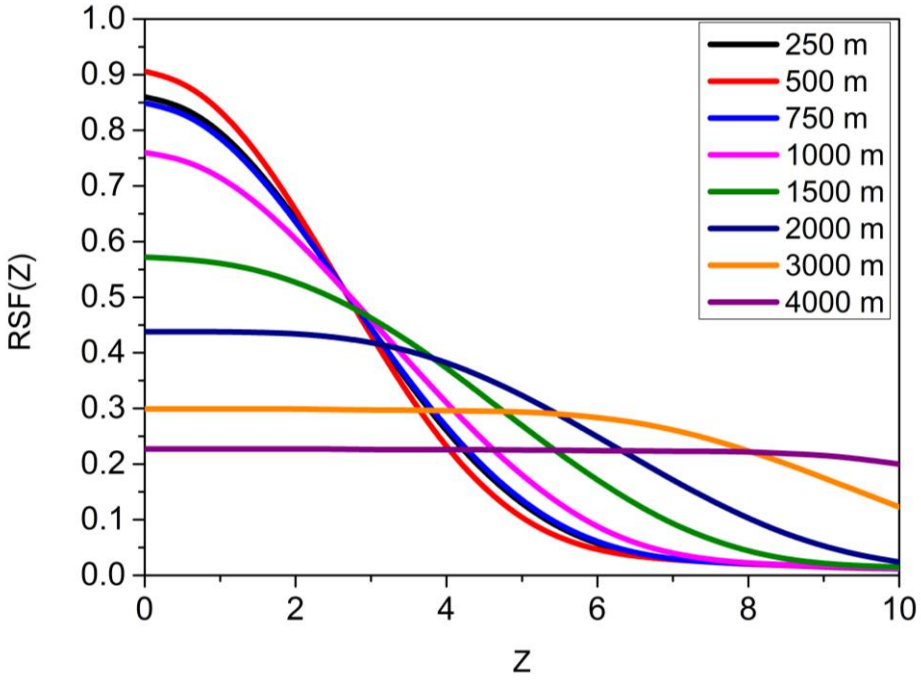

Figure 5. The intensity distribution of the detected thermal image of a vehicle moving at 80 Km/h for a system operating with a square aperture.

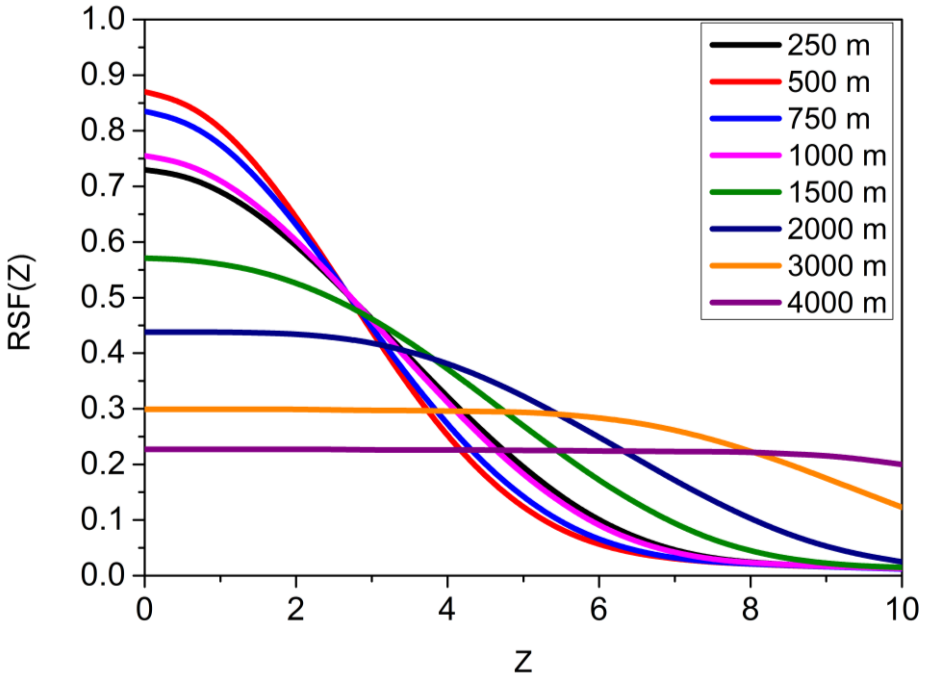

Figure 6. The intensity distribution of the detected thermal image of a vehicle moving at 120 Km/h for a system operating with a square aperture.

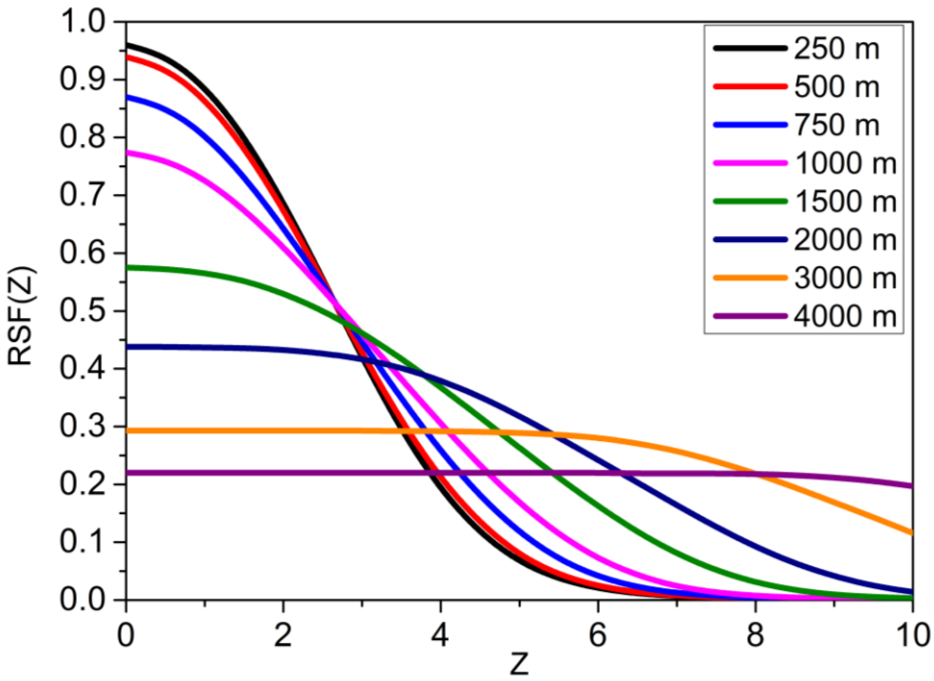

Figure 7. The intensity distribution of the detected thermal image of a vehicle moving at 40 Km/h for a system operating with a triangular aperture.

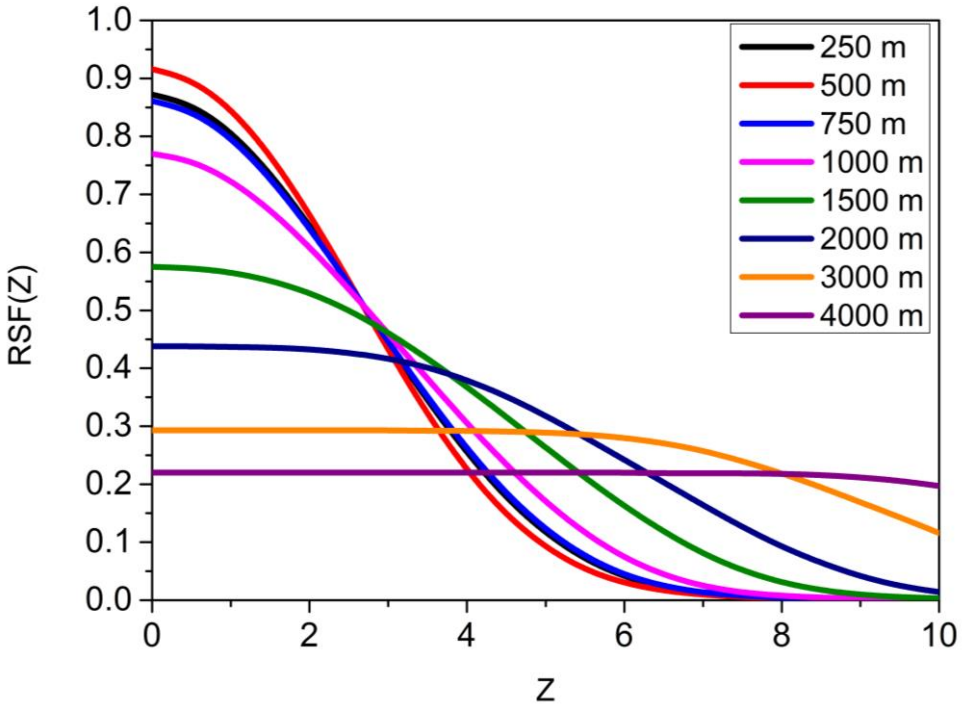

Figure 8. The intensity distribution of the detected thermal image of a vehicle moving at 80 Km/h for a system operating with a triangular aperture.

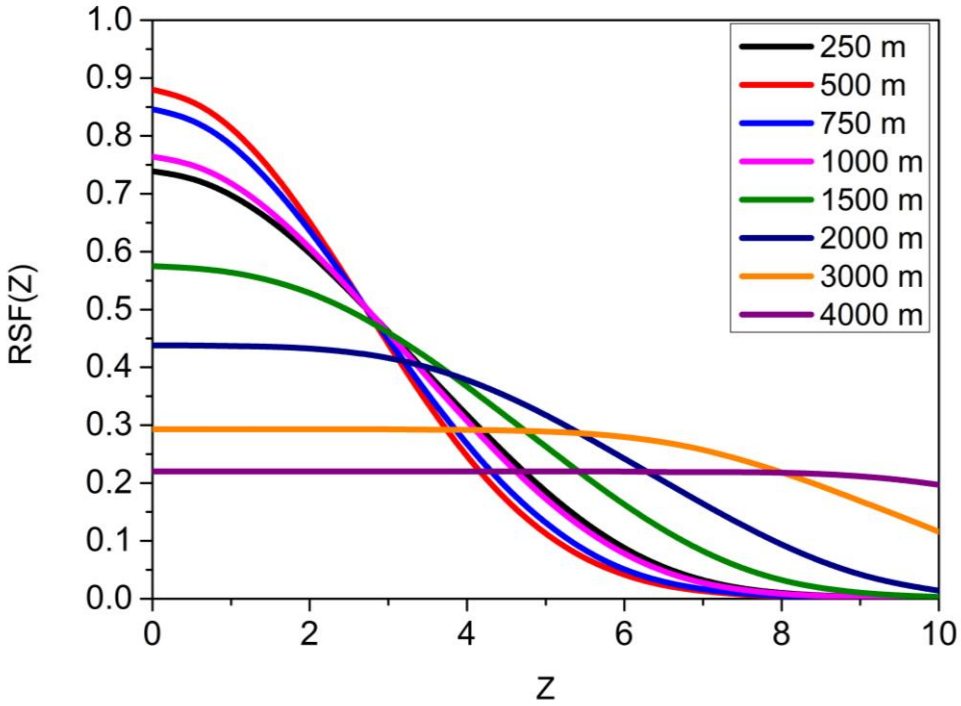

Figure 9. The intensity distribution of the detected thermal image of a vehicle moving at 120 Km/h for a system operating with a triangular aperture.

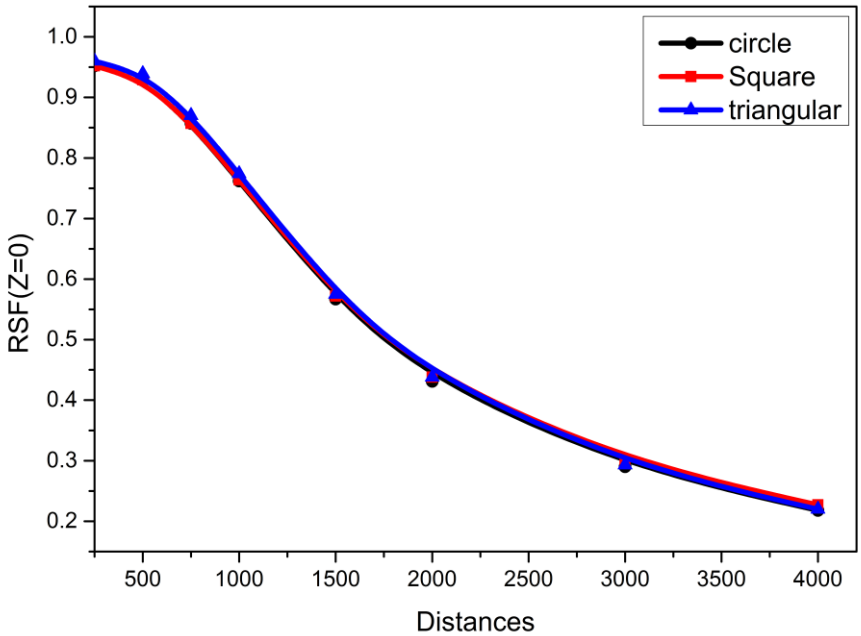

Figure 10. The maximum intensity of the detected thermal image for a vehicle moving at 40 Km/h at different distances and for different apertures.

Table 1: A comparison between the maximum intensity of RSF(z=0) at 40 Km/h for different apertures.

RSF(z=0)	At 250m	At 500m	At 750m	At 1km	At 1.5km	At 2km	At 3km	At 4km
Circular	0.952	0.929	0.857	0.762	0.567	0.431	0.290	0.218
Square	0.952	0.929	0.857	0.764	0.572	0.438	0.299	0.227
Triangular	0.96	0.939	0.87	0.774	0.575	0.438	0.293	0.22

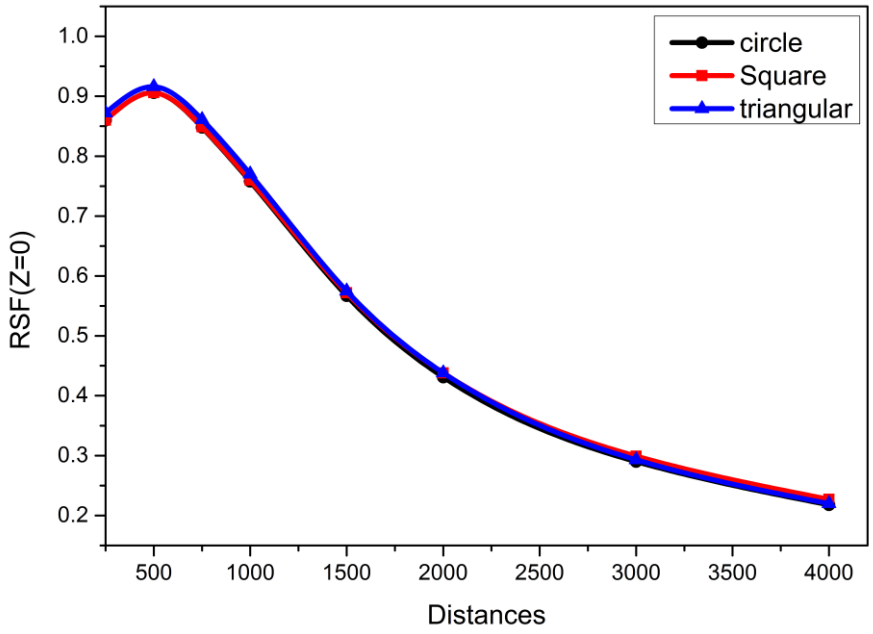

Figure 11. The maximum intensity of the detected thermal image for a vehicle moving at 80 Km/h at different distances and for different apertures.

Table 2: A comparison between the maximum intensity of RSF(z=0) at 80 Km/h for different apertures.

RSF(z=0)	At 250m	At 500m	At 750m	At 1km	At 1.5km	At 2km	At 3km	At 4km
Circular	0.86	0.906	0.848	0.758	0.567	0.431	0.29	0.218
Square	0.86	0.906	0.849	0.76	0.572	0.438	0.299	0.227
Triangular	0.872	0.916	0.861	0.77	0.575	0.438	0.293	0.22

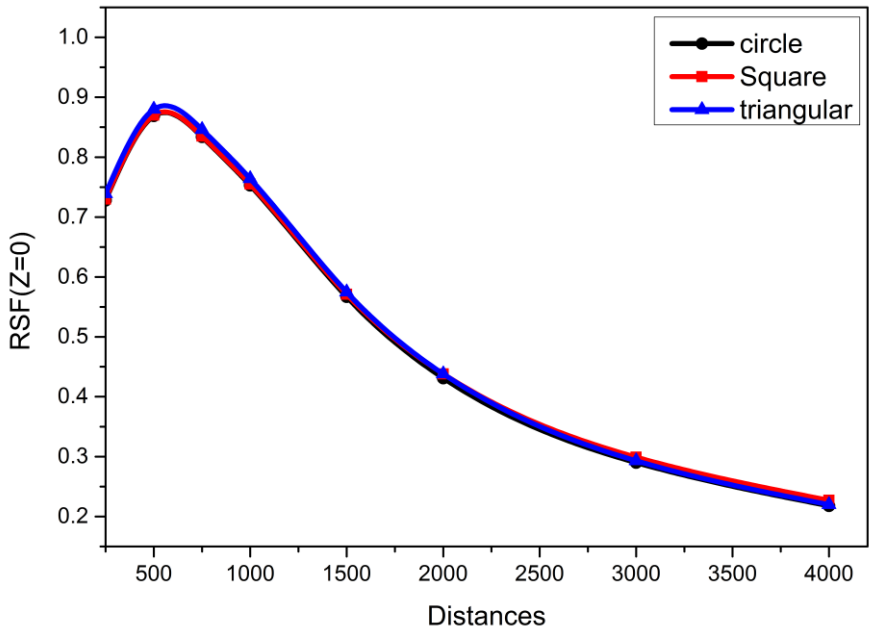

Figure 12. The maximum intensity of the detected thermal image for a vehicle moving at 120 Km/h at different distances and for different apertures.

Table 3: A comparison between the maximum intensity of RSF(z=0) at 120 Km/h for different apertures.

RSF(z=0)	At 250m	At 500m	At 750m	At 1km	At 1.5km	At 2km	At 3km	At 4km
Circular	0.728	0.869	0.834	0.753	0.567	0.431	0.29	0.218
Square	0.73	0.87	0.835	0.755	0.571	0.438	0.299	0.227
Triangular	0.739	0.88	0.846	0.764	0.575	0.438	0.293	0.22

CONCLUSION

In this work, a new mathematical model has been calculated for the first time, defined as the rectangular spread function for an object that simulates the shape of vehicles.

The effect of the linear motion was included in the equation of RSF to investigate the effect of velocity on the intensity distribution of the detected thermal image. The velocity of the object at (40, 80, and 120 Km/h) were considered at different distances between the thermal camera and the object (250,500, 750, 1000, 1500, 2000, 3000, and 4000 m). To find out which of these apertures has a better detected thermal image an optical system that studied working with three apertures (circular, square, and triangular).

From the results, a good detection range with a high-resolution thermal image is obtained at ranges of (250-1000) m. Above this range, particularly at (1000-2000) m, the thermal image becomes a blur and the target can detect but cannot recognize. At a range of more than 2000 m is impossible to detect and recognize the target in the thermal camera. The linear motion of objects (velocity) is a very important parameter that affects the intensity distribution of the detected thermal image. For the selected linear motion values, high speed of the target the intensity value of RSF reduces and thus, the accuracy of the detected thermal image decreases. The best detection of the thermal image is obtained for the target moving at a speed of 40 Km/h. Through the obtained results, the three apertures, that were studied, have a good efficiency to detect the thermal image. The detected thermal image, for the optical system, works using a circular, square, or triangular optical aperture and is affected by increasing the distance and the speed of the object. Additionally, there is no significant difference in the intensity value of the detected thermal image for the three different apertures. Likewise, the triangular optical

aperture is considered the best aperture in distances of less than 1.5 Km.

REFERENCES

[1] B. Jähne, *Applications and tools*, Digit. Image Process. 3 (2005).

[2] M. Rai, T. Maity, und R. K. Yadav, *Thermal imaging system and its real time applications: a survey*, J. Eng. Technol. **6**, 290 (2017).

[3] K. J. Havens und E. J. Sharp, *Thermal Imaging Techniques to Survey and Monitor Animals in the Wild: A Methodology* (Academic Press, 2015).

[4] D. J. McCafferty, *Applications of thermal imaging in avian science*, Ibis (Lond. 1859). **155**, 4 (2013).

[5] J. Zeng, L. Lin, und F. Deng, *Infrared thermal imaging as a nonradiation method for detecting thermal expression characteristics in normal female breasts in China*, Infrared Phys. Technol. **104**, 103125 (2020).

[6] A. F. A. Raheem, A. A. Raheem, und F. K. Fuliful, *Investigation of thermal imaging under bad weather conditions*, in *AIP Conference Proceedings*, Bd. 2386 (AIP Publishing LLC, 2022), S. 70004.

[7] A. A. Kharnoob und A. F. Hassan, *Effect of hexagonal synthetic aperture on the optical system with focal error*, J. Phys. Conf. Ser. **012047**, (2021).

[8] W. Fadl, *Design Optical Modulator by Using Fractal Function Geometry*.

[9] M. Venkanna und D. K. Sagar, *Amplitude filters in shaping the point spread function of optical imaging systems*, Proc. SPIE 9654, Int. Conf. Opt. Photonics 2015, 96540A (15 June 2015) (2022).

[10] A. A. Kharnoob und A. F. Hassan, *The effect of focal error on the point spread function for hexagonal aperture*, AIP Conf. Proc. **020021**, (2022).

[11] A. B. H. Al-Jizany, *Studying Of Image Intensity Distribution Of Elliptical Object (Elliptical Spread Function)*, AL- HAITHAM J. PURE APPL. SCI **2**, (2009).

[12] A.A.Raheem, *Study the Image of Line Object for Optical System Using Synthetic Circular Aperture*, J. kerbala Univ. **7**, (2009).

[13] A. F. A. Raheem, A. A. Raheem, und F. K. Fuliful, *Detection and analyzing the quality of thermal imager for moving object at different ranges*, in *AIP Conference Proceedings*, Bd. 2414 (AIP Publishing LLC, 2023), S. 30016.

[14] A. F. A. Raheem, A. A. Raheem, und F. K. Fuliful, *Investigation of IR atmospheric transmission under different concentrations of particulate matter PM10*, in *AIP Conference Proceedings*, Bd. 2547 (AIP Publishing LLC, 2022), S. 30008.

[15] A. B. H. Al-Jizany, *A. B. H. Al-Jizany, Studying Of Image Intensity Distribution Of Elliptical Object (Elliptical Spread Function)*, Ibn AL-Haitham J. Pure Appl. Sci. **22**, (2017).

[16] K. Singh, R. Rattan, und N. K. Jain, *Diffraction images of truncated sine and square wave periodic objects in the presence of linear image motion*, Appl. Opt. **12**, 1846 (1973).